Frontiers in Bioscience Landmark

Front. Biosci. (Landmark Ed) **2023**; 28(9): 217
https://doi.org/10.31083/j.fbl2809217

Original Research

Downregulation of CRTAC1 in Urothelial Carcinoma Promotes Tumor Aggressiveness and Confers Poor Prognosis

Wei-Ming Li[1,2,3,4], Ti-Chun Chan[5,6], Yu-Ching Wei[7,8], Chien-Feng Li[5,6,9], Hung-Lung Ke[1,2,10], Wen-Jeng Wu[1,2], Chin-Chia Hsu[11,*], Shao-Chuan Wang[12,13,*], Cheng-Fa Yeh[14,15,*]

[1]Department of Urology, Kaohsiung Medical University Hospital, 807 Kaohsiung, Taiwan
[2]Department of Urology, School of Medicine, College of Medicine, Kaohsiung Medical University, 807 Kaohsiung, Taiwan
[3]Department of Urology, Kaohsiung Medical University Gang-Shan Hospital, 807 Kaohsiung, Taiwan
[4]Department of Urology, Ministry of Health and Welfare Pingtung Hospital, 900 Pingtung, Taiwan
[5]Department of Medical Research, Chi Mei Medical Center, 710 Tainan, Taiwan
[6]National Institute of Cancer Research, National Health Research Institutes, 350 Miaoli, Taiwan
[7]Department of Pathology, School of Medicine, College of Medicine, Kaohsiung Medical University, 807 Kaohsiung, Taiwan
[8]Department of Pathology, Kaohsiung Municipal Ta-Tung Hospital, 801 Kaohsiung, Taiwan
[9]Department of Clinical Medicine, Chi Mei Medical Center, 710 Tainan, Taiwan
[10]Department of Urology, Kaohsiung Municipal Ta-Tung Hospital, 801 Kaohsiung, Taiwan
[11]Department of Chinese Medicine, Chi Mei Medical Center, 710 Tainan, Taiwan
[12]Department of Urology, Chung Shan Medical University Hospital, 402 Taichung, Taiwan
[13]School of Medicine, Chung Shan Medical University, 402 Taichung, Taiwan
[14]Division of General Internal Medicine, Chi Mei Medical Center, 710 Tainan, Taiwan
[15]Department of Environment Engineering and Science, Chia Nan University of Pharmacy and Science, 717 Tainan, Taiwan
*Correspondence: b97b02035@gmail.com (Chin-Chia Hsu); rosenbeck.wang@gmail.com (Shao-Chuan Wang); u802091@gmail.com (Cheng-Fa Yeh)
Academic Editor: Taeg Kyu Kwon
Submitted: 16 March 2023 Revised: 24 May 2023 Accepted: 20 June 2023 Published: 24 September 2023

Abstract

Background: Cartilage acidic protein 1 (CRTAC1) is a glycosylated calcium-binding extracellular matrix protein. The oncological functions of CRTAC1 in urothelial carcinoma (UC) of the urinary bladder (UB) and upper urinary tract (UT) have not yet been elucidated. Based on the published UBUC transcriptome data, we re-evaluated the differential expression profile of calcium ion binding–related genes (GO:0005509), and we found that *CRTAC1* was the most significantly downregulated gene in UBUC progression. Therefore, we analyzed the prognostic value and biological significance of CRTAC1 expression in UC. **Methods**: We used immunohistochemistry to determine the CRTAC1 expression levels in 340 patients with UTUC and 295 patients with UBUC. The CRTAC1 expression was compared with the clinicopathological characteristics, and the prognostic impact of CRTAC1 on metastasis-free survival (MFS) and disease-specific survival (DSS) was evaluated. To study the biological functions of CRTAC1, the proliferation, migration, invasion, and tube formation abilities of UC-derived cells were evaluated. **Results**: A low CRTAC1 expression significantly correlated with high tumor stage, high histological grade, perineural invasion, vascular invasion, nodal metastasis, and high mitotic rate (all $p < 0.01$). Moreover, the CRTAC1 immunoexpression status was an independent prognostic factor for MFS and DSS in UBUC and UTUC patients (all $p < 0.001$) in the multivariate analysis. The exogenous expression of CRTAC1 suppressed the cell proliferation, invasion, and angiogenesis, and downregulated the matrix metallopeptidase 2 (MMP2) level in BFTC909 and T24 cells. **Conclusions**: CRTAC1 may participate in progression of UC and serve as a prognostic marker for metastasis. Low CRTAC1 expression was significantly associated with aggressive UC characteristics and worse clinical outcomes. The inclusion of CRTAC1 immunoexpression in the standard pathological variables may optimize the risk stratification of patients.

Keywords: urothelial carcinoma; bladder cancer; UTUC; CRTAC1; prognosis

1. Introduction

Urothelial carcinomas (UCs) are the most common tumors of the urinary system diagnosed worldwide [1,2]. They can be located in the urethra, urinary bladder, ureter, or renal pelvis. The majority of UC cases are urinary bladder UC (UBUC), while upper urinary tract UC (UTUC) accounts for only 5%–10% of UCs [3–5]. The high histological and genetic heterogeneity of UC remains a clinical challenge [6,7]. For UTUC, radical nephroureterectomy (RNU) is the standard treatment for high-risk diseases; kidney-sparing surgery is recommended for patients with low risk UTUTC or serious renal insufficiency [5]. For UBUC, most patients receive transurethral resection of the bladder tumor (TURBT) for non-muscle-invasive bladder cancer (NMIBC), followed by intravesical instillations [3]. Radical cystectomy with perioperative chemotherapy is recommended for patients with muscle-invasive bladder cancer (MIBC) or high risk NMIBC [3,4]. Advances in therapeu-

tic modalities, surgical techniques, and health care systems have improved disease management strategies. However, the overall prognosis remains unsatisfactory [2–5]. Therefore, understanding the mechanisms underlying UC progression is critical for improving patient stratification and disease management.

Calcium (Ca^{2+}) is a secondary messenger that regulates several diverse biological and pathological processes in cells [8]. Dysregulation of calcium signaling is associated with tumorigenesis and cancer progression [9]. Some cellular functions are mediated by calcium-binding proteins [10]. Several calcium-binding proteins are known to play essential roles for urinary calcium oxalate stone formation processes [11]. However, the roles of calcium-binding proteins in the development of UC have not been investigated much. To better understand the significances of calcium-binding proteins in UC tumorigenesis, we used a public UC transcriptomic dataset (GSE32894) to investigate the differentially expressed genes (DEGs) related to the molecular function of calcium ion binding (GO:0005509). *CRTAC1* (cartilage acidic protein 1) was the most downregulated gene associated with UC progression.

CRTAC1, which is a glycosylated extracellular matrix (ECM) protein, is found in human articular cartilage [12]. Arg-Gly-Asp (RGD) integrin-binding motifs and Phe-Gly (FG) with Gly-Ala-Pro (GAP) (FG-GAP) motifs play significant roles in cell-matrix and cell-cell interactions [11]. In human dermal fibroblasts, CRTAC1 is involved in ECM development; organization, remodeling, and degradation of collagen; wound healing; and cellular regeneration, migration, and proliferation [13,14]. In human lens epithelial cells, upregulation of CRTAC1 promotes ultraviolet B-induced pyroptosis and cataract formation via reactive oxygen species signaling [15,16]. In osteoarthritis patients, CRTAC1 is an important regulator and its expression is induced by upregulation of IL-1β and TNF-α, resulting in the promotion of catabolism and inhibition of the anabolic activities of chondrocytes [17]. In bladder cancer, Yang *et al.* [18] demonstrated that CRTAC1 inhibited cell proliferation, migration, and invasion by targeting Yin Yang 1 to inactivate the TGF-β pathway. He *et al.* [19] found TFAP2A promoted TPRG1-AS1 transcription to reduce CRTAC1 expression, thereby accelerating bladder cancer cells glycolysis and angiogenesis. Using public bladder cancer datasets, Wang *et al.* [20] constructed a prognostic model based on the cuproptosis subtype-related prognostic differentially expressed genes, which included eight gene predictors (*PDGFRB*, *COMP*, *GREM1*, *FRRS1*, *SDHD*, *RARRES2*, *CRTAC1*, and *HMGCS2*). These studies only evaluated the function of CRTAC1 in UBUC, the possible role of CRTAC1 in UTUC has not yet been elucidated. Therefore, we assessed the prognostic values of CRTACI in UTUC and UBUC, and we investigated the functions and mechanisms of CRTACI in UC progression.

2. Materials and Methods

2.1 Data Mining

We performed transcriptomic profiling of a Gene Expression Omnibus (GEO) dataset (GSE32894) composing of 308 UBUC patients [21]. All probes without filtering or preselection were analyzed, and the raw data were imported into the Nexus Expression 3.0 (BioDiscovery, El Segundo, CA, USA) to compute gene abundances, as described in our previous study [22]. A comparative analysis (noninvasive vs. invasive UC) was performed to examine the DEGs related to calcium ion binding (GO:0005509). Those with a significant $\log_2$-transformed expression fold change <-0.15 ($p < 0.01$) were selected for further analysis.

2.2 Study Population

A total of 340 UTUC and 295 UBUC patients who underwent curative surgery between 1998 and 2004 were enrolled in the study, and all specimens were procured from our biobank after obtaining informed consent. The patients' clinical demographic characteristics, pathological features, and survival outcomes were retrospectively reviewed from their medical charts. None of the patients had undergone preoperative radiotherapy or chemotherapy. Postoperative platinum -based adjuvant chemotherapy was administered to patients with nodal involvement or pT3–pT4 diseases. The pathological grade and tumor stage were determined based on the WHO classification criteria and the 7th edition of the american joint committee on cancer (AJCC) staging system, respectively. The Institutional Review Board of Chi Mei Medical Center approved this study (10501005).

2.3 Immunohistochemical Assessments

Paraffin-embedded tissue blocks were sliced (4 µm) and placed on silane-coated slides, as previously described [22]. Deparaffinization, rehydration, and antigen retrieval were performed according to the standard procedures. The endogenous peroxidase activity was blocked using 3% H_2O_2 (ab64218, Abcam, Cambridge, England). The slides were then incubated with primary antibodies against CRTAC1 (1:100, ab254691, Abcam, Cambridge, England), matrix metallopeptidase 2 (MMP2) (1:100, ab86607, Abcam), or CD31 (1:100, ab28364, Abcam) for one hour. The target proteins were detected using a ChemMate™ EnVision™ Kit (Dako, Carpinteria, CA, USA). Positive CRTAC1 expression was characterized by membranous and/or cytoplasmic staining in UC cells. Sections processed without the primary anti-CRTAC1 antibody were used as negative controls. Two independent pathologists estimated the cancer cell distribution and the intensity of the immunohistochemical (IHC) staining to generate an H-score using the formula ΣPi(i + 1), where Pi is the percentage of stained cancer cells (0%–100%) and i is the intensity of the stained cancer cells (0–3+). The immunoreactivity of CRTAC1 was described as low or high levels of expression according to the median H-score,. As previously described, we iden-

tified the CD31-labeled vessels and used ImageJ software to calculate the tumoral microvessel density (MVD) [23].

2.4 Cell Culture

Five human UC-derived cell lines, namely TCCSUP (American Type Tissue Culture Collection [ATCC], VA), J82 (ATCC, VA), T24 (ATCC, VA), BFTC905 (Food Industry Research and Development Institute [FIRDI], Taiwan), and BFTC909 (FIRDI, Taiwan), were screened for CRTAC1 expression. A non-tumoral uroepithelial cell line, SV-HUC-1 (ATCC, VA), was used as a control. BFTC909 and T24 cells, which exhibit relatively low levels of endogenous CRTAC1, were selected for this study. These cells were cultured as previously described [24]. All cells were incubated at 37 °C in a humidified incubator containing 5% CO_2. The cell lines were regularly tested for mycoplasma and were authenticated by short tandem repeat genotyping.

2.5 Exogenous CRTAC1 Overexpression in T24 and BFTC909 Cells

The Phoenix-Amphotropic (AMPHO) cell line (ATCC, VA) was used to produce lentiviral particles containing *CRTAC1*. Briefly, the expression plasmids for CRTAC1 and the control vector (pLenti-GIII-CMV) were purchased from Applied Biological Materials, Inc (Richmond, BC, Canada). Following a series of transfections, as described previously [24], T24 and BFTC909 were incubated with culture medium containing viral supernatant and 10 µg/mL polybrene for 24 hours. Afterward, medium containing viral solution was replaced with fresh medium. UC cell lines overexpressing CRTAC1 were obtained as stable clones after puromycin selection (2 µg/mL).

2.6 Real-Time Quantitative RT-PCR

Total RNA was extracted from the UC cells using a Quick-RNA™ Miniprep Kit (Zymo Research, Beijing, China), and was reverse-transcribed using a Maxima First Strand cDNA Synthesis Kit (Thermo Scientific, Waltham, MA, USA). The cDNA was mixed with the corresponding TaqMan assay probes (*CRTAC1*, Hs00907892_m1; *MMP2*, Hs01548727_m1; *MMP9*, Hs00957562_m1; *POLR2A*, Hs01108291_m1; Applied Biosystems) using TaqMan™ Fast Advanced Master Mix (Thermo Scientific). We then performed quantitative RT-PCR for the mRNA level by the $2^{-\Delta\Delta CT}$ method using a StepOnePlus™ System (Applied Biosystems, Waltham, MA, USA). The relative expression levels of the target mRNAs were normalized to those of *POLR2A* RNA.

2.7 Western Blot Assays

We used PRO-PREP™ Protein Extraction Solution (iNtRON Biotechnology, Seongnam-Si, Gyeonggi-do, Republic of Korea) to extract total cellular proteins. The protein concentration was determined by a BCA assay kit (Thermo Fisher Scientific). Thirty micrograms of protein were loaded on an mPAGE Bis-Tris Precast Gel (Merck Millipore, Burlington, MA, USA) and transferred onto an Immobilon®-P PVDF membrane (Merck Millipore). The PVDF membranes were blocked with 5% skim milk (Millipore Sigma, Hong Kong, China) incubated overnight at 4 °C with the following primary antibodies: anti-CRTAC1 (ab254691, Abcam), anti-MMP2 (ab86607, Abcam), or anti-GAPDH (ab181602, Abcam). GAPDH served as an internal control. After washing, the membrane was incubated with a diluted secondary antibody (horseradish peroxidase [HRP] donkey anti-rabbit immunoglobulin G, BioLegend) for one hour. CRTAC1, MMP2, and GAPDH were visualized by enhanced chemiluminescence (Thermo Scientific).

2.8 Cell Proliferation Assay

Cell proliferation was evaluated using a Cell Proliferation Assay Kit (Fluorometric; BioVision, Hong Kong, China). Briefly, 1000 cells were pleated in 96-well microplates and incubated for 24, 48, and 72 h at 37 °C. Subsequently, 25 µL of the reaction mixture, including 1× nuclear dye/cell lysis buffer solution and 1× nuclear dye, was added to each well. After 15 min of incubation, the fluorescence intensity was determined using a standard microplate reader (excitation/emission = 480/538 nm). The assays were repeated at least three times.

2.9 Migration and Invasion Assays

The Boyden chamber technique (Transwell® analysis, Thermo Scientific, Hong Kong, China) was used to determine the cell migration and invasion abilities [25]. Cell migration and invasion assays were performed using Falcon HTS FluoroBlok 24-well inserts (BD Biosciences, Franklin Lakes, NJ, USA) and a QCM™ Collagen Cell Invasion Assay (Millipore), respectively. Each insert was rehydrated with serum-free medium and 1×10^6 UC cells suspended in serum-free medium were plated in the upper chamber and incubated with medium containing 10% FBS in the lower chamber. After 12–24 h of incubation, migrating and invading cells passing through the inserts were detached, stained with the provided dye and transferred to 96-well plates for colorimetric analysis at 560 nm. The assays were repeated at least three times.

2.10 In Vitro Tube Formation Assay

Human umbilical vein endothelial cells (HUVECs) were used to investigate the effects of CRTAC1 on UC-induced angiogenesis. The Matrigel® Matrix (Corning, Tewksbury, MA, USA) was used to precoat each inner well of the µ-Slide Angiogenesis (Ibidi, Gräfelfing, Germany) for 30 min at 37 °C. Then, 50 µL of cell suspension containing 7×10^3 HUVECs in 25 µL conditioned medium and 25 µL endothelial cell medium with 2% FBS was seeded on top of the Matrigel®. After incubation for 5 h at 37 °C, the capillary-like tube structures were evaluated and counted under a phase contrast microscope. The assays were repeated at least three times.

Table 1. Genes belonging to molecular function of calcium ion binding (GO:0005509) and showing significant stepwise down-regulation during progression in UC (GSE32894).

Probe	Comparing T1 to Ta		Comparing T2 to T1		Comparing T2 to Ta		Gene Title	Molecular Function
	log ratio	*p* value	log ratio	*p* value	log ratio	*p* value		
ILMN_1658384	–1.9169	0	–1.4772	0	–3.3941	<0.0001	*CRTAC1*	calcium ion binding
ILMN_1671473	–0.149	0.0023	–0.1544	0.0009	–0.3034	<0.0001	*EHD3*	ATP binding, GTP binding, GTPase activity, calcium ion binding, nucleic acid binding, nucleotide binding, protein binding
ILMN_1677108	–0.4308	0.0015	–0.3607	0.0018	–0.7914	<0.0001	*CAPN13*	calcium ion binding, calcium-dependent cysteine-type endopeptidase activity, cysteine-type peptidase activity, peptidase activity
ILMN_1684873	–0.5354	<0.0001	–0.4178	0.0001	–0.9532	<0.0001	*ARSD*	arylsulfatase activity, calcium ion binding, catalytic activity, hydrolase activity, sulfuric ester hydrolase activity
ILMN_1690289	–0.5202	<0.0001	–0.4412	0.0001	–0.9615	<0.0001	*DUOX1*	FAD binding, NAD(P)H oxidase activity, NADP or NADPH binding, calcium ion binding, electron carrier activity, heme binding, iron ion binding, oxidoreductase activity, peroxidase activity
ILMN_1697597	–0.2378	0.0005	–0.2708	0.0006	–0.5086	<0.0001	*KIAA0494*	calcium ion binding
ILMN_1699421	–2.3186	<0.0001	–0.8656	0.0007	–3.1842	<0.0001	*ANXA10*	calcium ion binding, calcium-dependent phospholipid binding
ILMN_1699809	–0.997	<0.0001	–0.5255	0.0019	–1.5225	<0.0001	*CAPNS2*	calcium ion binding
ILMN_1722798	–0.5597	<0.0001	–0.4854	<0.0001	–1.045	<0.0001	*PLCD3*	calcium ion binding, hydrolase activity, phosphoinositide phospholipase C activity, signal transducer activity
ILMN_1738707	–0.1485	0.0022	–0.1534	0.0085	–0.3019	<0.0001	*S100A13*	calcium ion binding
ILMN_1744211	–0.3374	0.0008	–0.371	0.0001	–0.7085	<0.0001	*PLA2G4F*	calcium ion binding, hydrolase activity, phospholipase A2 activity, phospholipase activity
ILMN_1744517	–0.1788	0.0068	–0.1884	0.0034	–0.3673	<0.0001	*GNS*	N-acetylglucosamine-6-sulfatase activity, calcium ion binding, hydrolase activity
ILMN_1747395	–0.3836	<0.0001	–0.3163	<0.0001	–0.6999	<0.0001	*SLC24A1*	antiporter activity, calcium ion binding, calcium; potassium:sodium antiporter activity, symporter activity
ILMN_1750181	–0.5849	0.0081	–1.2709	<0.0001	–1.8558	<0.0001	*TESC*	calcium ion binding, magnesium ion binding, phosphatase inhibitor activity, protein binding
ILMN_1757660	–0.4278	0.0032	–0.6223	<0.0001	–1.0501	<0.0001	*CAPS*	calcium ion binding
ILMN_1758888	–0.6624	0.0022	–0.5401	0.0023	–1.2026	<0.0001	*PADI3*	calcium ion binding, hydrolase activity, protein-arginine deiminase activity
ILMN_1763198	–0.2438	0.0005	–0.2579	0.0039	–0.5017	<0.0001	*STAT6*	calcium ion binding, protein binding, sequence-specific DNA binding, signal transducer activity, transcription factor activity
ILMN_1775114	–0.469	0.0003	–0.6834	<0.0001	–1.1524	<0.0001	*ENTPD3*	calcium ion binding, hydrolase activity, magnesium ion binding, nucleoside-diphosphatase activity, nucleoside-triphosphatase activity
ILMN_1779401	–0.4247	<0.0001	–0.2361	0.001	–0.6608	<0.0001	*CHP*	calcium ion binding, potassium channel regulator activity
ILMN_1785175	–0.3426	0.0003	–0.245	0.003	–0.5876	<0.0001	*SWAP70*	ATP binding, DNA binding, calcium ion binding, protein binding
ILMN_2061565	–0.6809	0	–0.4995	0.0005	–1.1804	<0.0001	*PLCH2*	calcium ion binding, hydrolase activity, molecular_function, phosphoinositide phospholipase C activity, signal transducer activity
ILMN_2087941	–0.6462	<0.0001	–0.7558	<0.0001	–1.402	<0.0001	*ENTPD3*	calcium ion binding, hydrolase activity, magnesium ion binding, nucleoside-diphosphatase activity, nucleoside-triphosphatase activity

Table 1. Continued.

Probe	Comparing T1 to Ta		Comparing T2 to T1		Comparing T2 to Ta		Gene Title	Molecular Function
	log ratio	*p* value	log ratio	*p* value	log ratio	*p* value		
ILMN_2319913	–0.3438	0.0005	–0.2817	0.0026	–0.6255	<0.0001	*DGKA*	calcium ion binding, diacylglycerol binding, diacylglycerol kinase activity, phospholipid binding, transferase activity, zinc ion binding
ILMN_2404182	–0.2449	0.0002	–0.1527	0.0097	–0.3976	<0.0001	*DUOX1*	FAD binding, NAD(P)H oxidase activity, NADP or NADPH binding, calcium ion binding, electron carrier activity, heme binding, iron ion binding, oxidoreductase activity, peroxidase activity

UC, urothelial carcinomas; FAD, flavin adenine dinucleotide.

Table 2. Correlations between CRTAC1 expression and other important clinicopathological parameters in urothelial carcinomas.

Parameter	Category	Upper Urinary Tract Urothelial Carcinoma				Urinary Bladder Urothelial Carcinoma			
		Case No.	CRTAC1 Expression		*p*-value	Case No.	CRTAC1 Expression		*p*-value
			Low	High			Low	High	
Gender	Male	158	75 (47.5)	83 (52.5)	0.384	216	112 (51.9)	104 (48.1)	0.251
	Female	182	95 (52.2)	87 (47.8)		79	35 (44.3)	44 (55.7)	
Age (years)	<65	138	75 (54.3)	63 (45.7)	0.185	121	63 (52.1)	58 (47.9)	0.522
	≥65	202	95 (47.0)	107 (53.0)		174	84 (48.3)	90 (51.7)	
Tumor location	Renal pelvis	141	74 (52.5)	67 (47.5)	0.157	-	-	-	-
	Ureter	150	67 (44.7)	83 (55.3)		-	-	-	-
	Renal pelvis ureter	49	29 (59.2)	20 (40.8)		-	-	-	-
Multifocality	Single	278	135 (48.6)	143 (51.4)	0.261	-	-	-	-
	Multifocal	62	35 (56.5)	27 (43.5)		-	-	-	-
Primary tumor (T)	Ta	89	16 (18.0)	73 (82.0)	<0.001*	84	27 (32.1)	57 (67.9)	<0.001*
	T1	92	35 (56.5)	57 (43.5)		88	30 (34.1)	58 (65.9)	
	T2–T4	159	119 (74.8)	40 (25.2)		123	90 (73.2)	33 (26.8)	
Nodal metastasis	Negative (N0)	312	144 (46.2)	168 (53.8)	<0.001*	266	124 (46.6)	142 (53.4)	0.001*
	Positive (N1–N2)	28	26 (92.9)	2 (7.1)		29	6 (20.7)	23 (79.3)	
Histological grade	Low grade	56	13 (23.2)	43 (76.8)	<0.001*	56	13 (23.2)	43 (76.8)	<0.001*
	High grade	284	157 (55.3)	127 (44.7)		239	134 (56.1)	105 (43.9)	
Vascular invasion	Absent	234	88 (37.6)	146 (62.4)	<0.001*	246	104 (42.3)	142 (57.7)	<0.001*
	Present	106	82 (77.4)	24 (22.6)		49	43 (87.8)	6 (12.2)	
Perineural invasion	Absent	321	154 (48.0)	167 (52.0)	0.002*	275	131 (47.6)	144 (52.4)	0.005*
	Present	19	16 (84.2)	3 (15.8)		20	16 (80.0)	4 (20.0)	
Mitotic rate (per 10 high power fields)	<10	173	60 (34.7)	113 (65.3)	<0.001*	139	57 (41.0)	82 (59.0)	0.004*
	≥10	167	110 (65.9)	57 (34.1)		156	90 (57.7)	66 (42.3)	
MMP2 expression	Low	223	86 (38.6)	137 (61.4)	<0.001*	190	73 (38.4)	117 (61.6)	<0.001*
	High	117	84 (71.8)	33 (28.2)		105	74 (70.5)	31 (29.5)	

* Statistically significant. MMP2, matrix metallopeptidase 2.

Table 3. Univariate log-rank and multivariate analyses for disease-specific and metastasis-free survivals in upper urinary tract urothelial carcinoma.

Parameter	Category	Case No.	Disease-specific Survival					Metastasis-free Survival				
			Univariate analysis		Multivariate analysis			Univariate analysis		Multivariate analysis		
			No. of events	*p*-value	HR	95% CI	*p*-value	No. of events	*p*-value	HR	95% CI	*p*-value
Gender	Male	158	28 (17.7)	0.8286	-	-	-	32 (20.3)	0.7904	-	-	-
	Female	182	33 (18.1)		-	-	-	38 (20.9)		-	-	-
Age (years)	<65	138	26 (18.8)	0.9943	-	-	-	30 (21.7)	0.8470	-	-	-
	≥65	202	35 (17.3)		-	-	-	40 (19.8)		-	-	-
Tumor side	Right	177	34 (19.2)	0.7366	-	-	-	38 (21.5)	0.3074	-	-	-
	Left	154	26 (16.9)		-	-	-	32 (20.8)		-	-	-
	Bilateral	9	1 (11.1)		-	-	-	0 (0.0)		-	-	-
Tumor location	Renal pelvis	141	24 (17.0)	0.0079*	1	-	0.769	31 (22.0)	0.0659	-	-	-
	Ureter	150	22 (14.7)		0.746	0.206–2.706		25 (16.7)		-	-	-
	Renal pelvis ureter	49	15 (30.6)		0.634	0.163–2.464		14 (28.6)		-	-	-
Multifocality	Single	273	48 (17.6)	0.0026*	1	-	0.369	52 (19.0)	0.0127*	1	-	0.235
	Multifocal	62	18 (29.0)		1.761	0.512–6.054		18 (29.0)		1.748	0.695–4.394	
Primary tumor (T)	Ta	89	2 (2.2)	<0.0001*	1	-	0.439	4 (4.5)	<0.0001*	1	-	0.529
	T1	92	9 (9.8)		2.383	0.489–11.626		15 (16.3)		1.278	0.659–2.479	
	T2–T4	159	50 (31.4)		2.773	0.583–13.196		51 (32.1)		1.353	0.792–2.309	
Nodal metastasis	Negative (N0)	312	42 (13.5)	<0.0001*	1	-	<0.001*	55 (17.6)	<0.0001*	1	-	<0.001*
	Positive (N1–N2)	28	19 (67.9)		4.644	2.393–9.012		15 (53.6)		2.720	1.571–4.707	
Histological grade	Low grade	56	4 (7.1)	0.0215*	1	-	0.084	3 (5.4)	0.0027*	1	-	0.524
	High grade	284	57 (20.1)		2.421	0.889–6.589		67 (23.6)		1.194	0.693–2.057	
Vascular invasion	Absent	234	24 (10.3)	<0.0001*	1	-	0.206	26 (11.1)	<0.0001*	1	-	0.131
	Present	106	37 (34.9)		1.483	0.805–2.731		44 (41.5)		1.433	0.898–2.287	
Perineural invasion	Absent	321	50 (15.6)	<0.0001*	1	-	<0.001*	61 (19.0)	<0.0001*	1	-	<0.001*
	Present	19	11 (57.9)		4.023	1.911–8.472		9 (47.4)		2.814	1.536–5.156	
Mitotic rate (per 10 high power fields)	<10	173	27 (15.6)	0.167	-	-		30 (17.3)	0.0823	-	-	
	≥10	167	34 (20.4)		-	-		40 (24.0)		-	-	
MMP2 expression	Low	223	27 (12.1)	<0.0001*	1		0.883	36 (16.1)	0.0020*			0.944
	High	117	34 (29.1)		0.956	0.522–1.751		34 (29.1)		1.015	0.674–1.527	
CRTAC1 expression	Low	170	55 (32.4)	<0.0001*	1	-	<0.001*	59 (34.7)	<0.0001*	1	-	<0.001*
	High	170	6 (3.5)		0.188	0.073–0.481		11 (6.5)		0.255	0.152–0.426	

* Statistically significant. HR, hazard ratio; CI, confidence interval.

Table 4. Univariate log-rank and multivariate analyses for disease-specific and metastasis-free survivals in urinary bladder urothelial carcinoma.

Parameter	Category	Case No.	Disease-specific Survival					Metastasis-free Survival				
			Univariate analysis		Multivariate analysis			Univariate analysis		Multivariate analysis		
			No. of events	*p*-value	HR	95% CI	*p*-value	No. of events	*p*-value	HR	95% CI	*p*-value
Gender	Male	216	41(19.0)	0.4446	-	-	-	61 (28.2)	0.2720	-	-	-
	Female	79	11 (13.9)		-	-	-	16 (20.3)		-	-	-
Age (years)	<65	121	17 (14.0)	0.1136	-	-	-	32 (26.4)	0.6875	-	-	-
	≥65	174	35 (20.1)		-	-	-	45 (25.9)		-	-	-
Primary tumor (T)	Ta	84	1 (1.2)	<0.0001*	1	-	<0.001*	4 (4.8)	<0.0001*	1	-	0.010*
	T1	88	9 (10.2)		3.787	1.704–8.418		23 (26.1)		4.131	1.296–13.173	
	T2–T4	123	42 (34.1)		18.898	2.413–148.007		50 (40.7)		5.967	1.866–19.083	
Nodal metastasis	Negative (N0)	266	41 (15.4)	0.0002*	1	-	0.553	61 (22.9)	<0.0001*	1	-	0.027*
	Positive (N1–N2)	29	11 (37.9)		1.245	0.603–2.570		16 (55.2)		2.009	1.084–3.724	
Histological grade	Low grade	56	2 (3.6)	0.0013*	1	-	0.570	5 (8.9)	0.0007*	1	-	0.938
	High grade	239	50 (20.9)		1.557	0.338–7.174		72 (30.1)		1.042	0.376–2.889	
Vascular invasion	Absent	246	37 (15.0)	0.0024*	1	-	0.033*	54 (22.0)	0.0001*	1	-	0.843
	Present	49	15 (30.6)		0.469	0.234–0.939		23 (46.9)		0.940	0.509–1.736	
Perineural invasion	Absent	275	44 (16.0)	0.0001*	1	-	0.024*	67 (24.4)	0.0007*	1	-	0.190
	Present	20	8 (40.0)		2.611	1.132–6.022		10 (50.0)		1.646	0.781–3.466	
Mitotic rate (per 10 high power fields)	<10	139	12 (8.6)	<0.0001*	1	-	0.150	23 (16.5)	<0.0001*	1	-	0.140
	≥10	156	40 (25.6)		1.655	0.834–3.287		54 (34.6)		1.472	0.881–2.460	
MMP2 expression	Low	190	22 (11.6)	0.0001*			0.593	35 (18.4)	<0.0001*	1		0.120
	High	105	30 (28.6)		1.175	0.651–2.119		42 (40.0)		1.462	0.906–2.360	
CRTAC1 expression	Low	147	43 (29.3)	<0.0001*	1	-	<0.001*	55 (37.4)	<0.0001*	1	-	<0.001*
	High	148	9 (6.1)		0.220	0.102–0.474		22 (14.9)		0.374	0.218–0.642	

* Statistically significant.

2.11 Luciferase Reporter Assays

The vector pcDNA3-CRTAC1 was constructed as previously described [26]. MMP2 and MMP9 promoter fragments were cloned by PCR amplification and inserted into a luciferase reporter gene plasmid vector (Promega, Fitchburg, WI, USA). The MMP2 and MMP9 promoter reporter constructs and pcDNA3-CRTAC1 construct or their matching empty constructs were co-transfected in cells using PolyJet^{TM} transfection reagent (SignaGen Laboratories, Shandong, China) for 48 h. We then used a Dual-Glo® Luciferase Reporter Assay System (Promega) to measure the luciferase activity following the manufacturer's protocol.

2.12 Statistical Analyses

Associations between CRTAC1 expression and different variables were evaluated using the chi-square test. For survival analyses, the disease-specific survival (DSS) and metastasis-free survival (MFS) were plotted using Kaplan–Meier curves and estimated using the log-rank test at the univariate level. The independent prognostic factors were estimated using a multivariate Cox proportional hazards model. All cellular functional studies were done with three replicates. Student's *t*-test was used to analyze differences in cell proliferation, migration, invasion, HUVEC tube formation, and luciferase activity. Statistical analyses were performed using SPSS 19 software (SPSS Inc., Chicago, IL, USA). In all analyses, a *p*-value of <0.05 was considered to reflect statistical significance.

3. Results

3.1 CRTAC1 is the Most Significantly Downregulated Gene Related to the Calcium Ion Binding in UBUC Invasiveness

We identified 34 probes covering 22 transcripts associated with calcium ion binding (GO:0005509) in UBUC invasion using a published transcriptome dataset (GSE32894). These genes were significantly downregulated at the high tumor stage (Fig. 1 and Table 1). C*RTAC1* was selected for further evaluation because it was the most downregulated gene. Using the Gene Expression Profiling Interactive Analysis database, *CRTAC1* was found to be significantly decreased in UBUC (n = 404) compared to in adjacent normal tissues (n = 19) ($p < 0.001$). Intriguingly, violin plots showed that *CRTAC1* mRNA levels significantly decreased as the UBUC stage increased (from stage II to IV). Moreover, UBUC patients with high *CRTAC1* mRNA expression had better overall survival than those with low *CRTAC1* mRNA expression ($p = 0.0007$) (**Supplementary Fig. 1**). These results prompted us to assess the prognostic value and clinical relevance of CRTAC1 in a large cohort of UC patients.

3.2 Demographic Features

In total, 635 patients (UTUC, 340; UBUC, 295) with a mean age of 65.8 years were included in this study (Table 2). In the UTUC cohort, the majority of patients (n = 284, 83.5%) had a high histological grade, 159 patients (46.8%) had advanced UTUC (pT2-pT4), and 28 patients (8.2%) had metastatic nodal disease at initial diagnosis. Forty-nine patients (14.4%) developed concurrent renal pelvic and ureteral tumors, while 62 (18.2%) developed multiple tumors. In addition, perineural invasion was detected in 19 patients (5.9%), while vascular invasion was detected in 106 patients (31.2%). The UBUC cohort comprised 239 (81.0%) patients with high histological grade tumors, 123 (41.7%) with advanced-stage disease (pT2–pT4), and 29 (7.8%) with metastatic lymph nodes. A total of 156 tumors (52.9%) exhibited high mitotic activity. Perineural invasion and vascular invasion were detected in 49 (16.6%) and 20 (6.8%) patients, respectively.

3.3 Association between CRTAC1 Expression and Clinicopathological Characteristics

Immunostaining was performed to evaluate CRTAC1 expression levels in the surgical tissue and revealed that invasive UC had lower CRTAC1 immunoreactivity than noninvasive UC (Fig. 2). The clinical significance of CRTAC1 expression in UC was also examined (Table 2). In the UTUC cohort, CRTAC1 expression significantly correlated with the tumor stage ($p < 0.001$), histological grade ($p < 0.001$), lymph nodal status ($p < 0.001$), vascular invasion ($p < 0.001$), perineural invasion ($p = 0.002$), and mitotic activity ($p < 0.001$). In the UBUC cohort, low CRTAC1 immunoexpression was associated with pT2–pT4 stage ($p < 0.001$), high histological grade ($p < 0.001$), nodal metastasis ($p < 0.001$), perineural invasion ($p = 0.005$), vascular invasion ($p < 0.001$), and a high mitotic rate ($p = 0.004$).

3.4 Prognostic Significance of CRTAC1 Expression

Within a median follow-up of 31.7 months, 70 UTUC and 76 UBUC patients developed tumor metastasis, while 61 UTUC and 52 UBUC patients died of UC.

Univariate and multivariate analyses were conducted to assess whether CRTAC1 expression affected cancer metastasis and death. With regard to UTUC (Table 3), 55 patients (29.1%) with low CRTAC1-expressing cancers died, while 59 patients (34.7%) subsequently developed cancer metastasis. Only 11 patients (6.5%) with high CRTAC1-expressing cancers developed metastatic cancers, while 9 patients (6.2%) died of UTUC. In particular, low CRTAC1-expressing tumors predicted worse DSS (Fig. 3A; $p < 0.0001$) and MFS (Fig. 3B; $p < 0.0001$) based on the results of the Kaplan-Meier survival analysis. In addition to CRTAC1 immunostaining status, multifocal tumors, advanced tumor stage, high histological tumor grade, nodal metastasis, and vascular and perineural invasion were significantly associated with inferior MFS and DSS. In the multivariate analysis, high CRTAC1 immunoactivity was clearly associated with better MFS and DSS (DSS: hazard ratio [HR]: 0.188, 95% confidence interval [CI]: 0.073–0.481, $p < 0.001$; MFS: HR: 0.255, 95% CI: 0.152–0.426, $p < 0.001$).

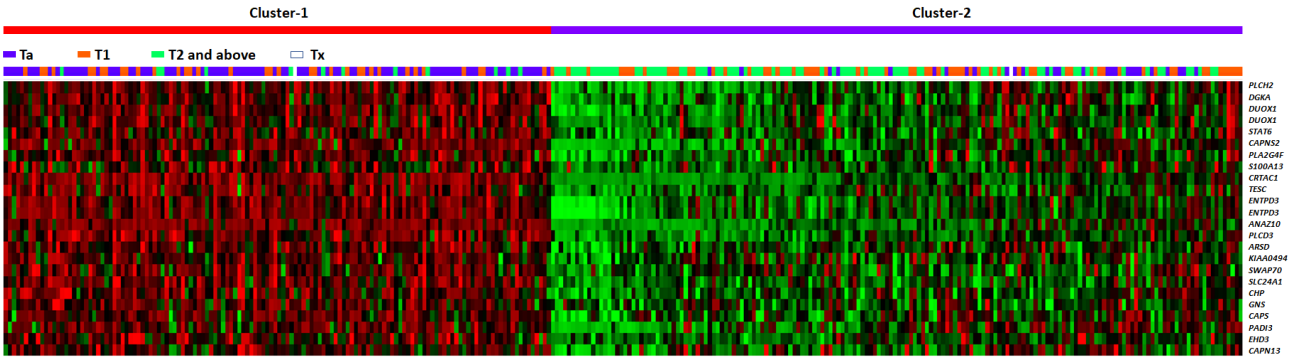

Fig. 1. Data mining. Expression profiles of genes associated with the calcium ion binding (GO:0005509) extracted from a published transcriptome of UC (GSE32894) in the Gene Expression Omnibus database. *CRTAC1* was the most downregulated gene associated with UC progression. UC, urothelial carcinoma.

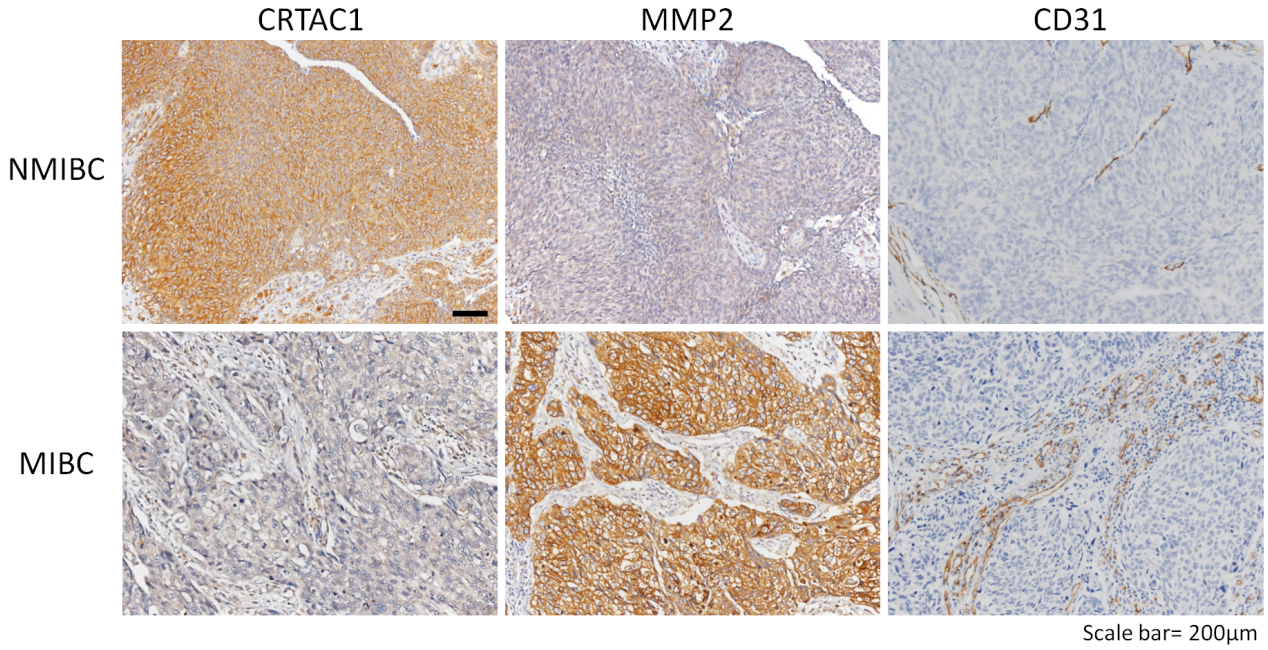

Fig. 2. Immunohistochemistry. Lower expression of CRTAC1 is associated with higher MMP2 expression, higher CD31-labeled microvascular density, and higher tumor stage in UC. (Scale bar = 200 μm) (CRTAC1, cartilage acidic protein 1; MMP2, matrix metallopeptidase 2; NMIBC, non-muscle invasive bladder cancer; MIBC, muscle invasive bladder cancer).

In UBUC (Table 4), low CRTAC1 expression levels were associated with higher rates of postoperative cancer metastasis (31.2% vs. 10.0%) and cancer-related deaths (27.1% vs. 8.8%) than high CRTAC1 expression levels. In Kaplan–Meier survival analysis, CRTAC1 immunoexpression (Fig. 3C,D), pT stage, tumor grade, perineural invasion, vascular invasion, lymph node status, and mitotic rate were significantly correlated with worse DSS and MFS. In addition, multivariate Cox regression analysis showed that CRTAC1 immunoexpression status was an independent prognosticator of cancer-related death (HR: 0.220, 95% CI: 0.102–0.474, $p < 0.001$) and metastasis occurrence (HR: 3.374, 95% CI: 0.218–0.642, $p < 0.001$).

3.5 CRTAC1 Inhibition of UC Cell Proliferation, Invasion, and Angiogenesis

To understand the biological function of CRTAC1, endogenous CRTAC1 expression in UC cell lines was determined. Compared to normal urothelial primary cells (SV-HUC-1), all five UC-derived cell lines had lower CRTAC1 mRNA and protein expression (Fig. 4A). Of these, BFTC909 and T24 cells exhibited the lowest levels of CRTAC1 expression; therefore, CRTAC1 overexpression was induced in these two cell lines (Fig. 4B). The overexpression of CRTAC1 in BFTC909 and T24 cells significantly attenuated cell proliferation (Fig. 4C). Matrigel® invasion assays indicated that CRTAC1 overexpression also significantly decreased the number of invading tumor cells, thus indicating its ability to inhibit metastasis (Fig. 4D). More-

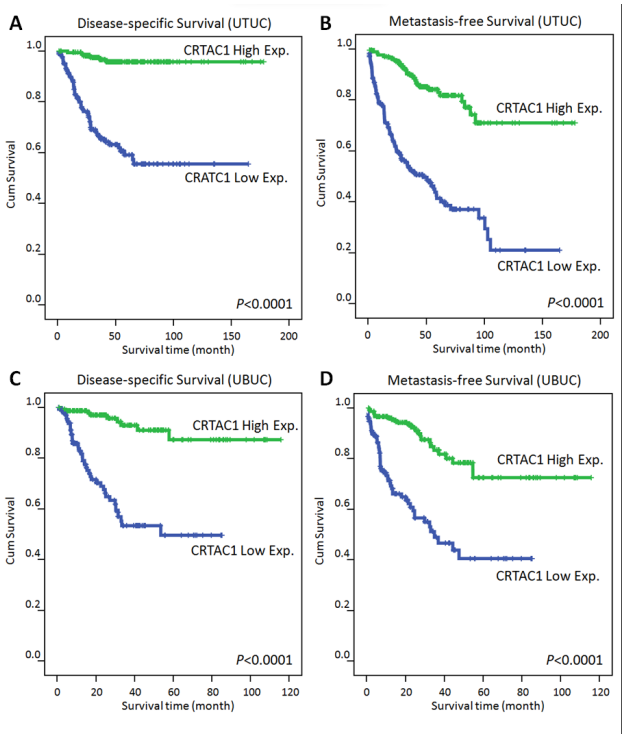

Fig. 3. Kaplan-Meier survival curves. Low CRTAC1 expression is associated with a significant prognostic impact on disease-specific survival and metastasis-free survival of patients with UTUC (A and B, respectively) and UBUC (C and D, respectively). UTUC, upper urinary tract urothelial carcinoma; UBUC, urinary bladder urothelial carcinoma.

over, conditioned medium from CRTAC1-overexpressing BFTC909 and T24 cells markedly inhibited HUVEC tube formation compared to that in the mock group (Fig. 5A). In addition to *in vitro* studies, we studied the association between CRTAC1 and MVD in our UC specimens. Notably, high CRTAC1 expression was significantly correlated with less CD31-labeled MVD in UTUC and UBUC. (Fig. 5B) To identify the potential cellular pathways that are involved in the regulation of UC invasiveness by CRTAC1, MMP2 was selected for further studies. Initially, IHC staining showed that high CRTAC1 expression negatively correlated with low MMP2 expression in UTUC and UBUC (Table 2; Fig. 2). qRT-PCR and immunoblotting showed that exogenous CRTAC1 expression markedly suppressed MMP2 mRNA and protein expression in BFTC909 and T24 cells (Fig. 6A). Finally, analysis of luciferase activity driven by the MMP2 promoter showed that MMP2 transactivation was negatively associated with CRTAC1 expression in UC cells. These results confirm the role of MMP2 in CRTAC1-driven UC aggressiveness (Fig. 6B).

4. Discussion

UCs, including UTUC and UBUC, have genetic and clinical heterogeneity [6,7]. Despite the advances in treatment modalities and surgical techniques, patient survival rates remain poor. Therefore, the incorporation of genetic information may optimize the risk stratification of patients and disease management. Through transcriptomic profiling, we discovered that *CRTAC1* was the most downregulated calcium-ion-binding gene in UC. In the The Cancer Genome Atlas (TCGA) bladder cancer database, *CRTAC1* mRNA abundance in cancer tissues was lower than that in adjacent normal tissues. Its expression was notably decreased in patients with high stage cancer. These observations suggest that CRTAC1 acts as a tumor suppressor during UC progression. Accordingly, the clinical relevance of CRTAC1 was evaluated in our well-characterized UC cohorts. CRTAC1 expression was an independent prognostic factor for MFS and DSS, after adjusting for important pathological parameters. Patients with high CRTAC1 expression had significantly better clinical prognosis. Our study was the first to report an association between CRTAC1 expression and metastasis and survival in UBUC and UTUC.

CRTAC1, located on chromosome 10q24.2, encodes a glycosylated calcium-binding ECM protein called cartilage acidic protein 1 [12]. However, the functions of CRTAC1 reamin poorly understood. It contains a calcium-binding epidermal growth factor domain and an integrin alpha chain-like domain that interacts with ECM proteins and mediates cell-cell and cell-matrix interactions [12,27,28]. This protein was originally discovered during the chondrocyte development, and its concentration was relatively high in patients with osteoarthritis [11,16]. CRTAC1 also promotes apoptosis and pyroptosis in human lens epithelial cells resulting in cataract formation [15,29]. It regulates energy metabolism and promotes proliferation and migration in primary human dermal fibroblasts [14]. However, the role of CRTAC1 in UC tumorigenesis and progression remains unclear. Accordingly, its prognostic significance in large UBUC and UTUC cohorts was evaluated.

In UBUC, most patients with NMIBC underwent TURBT, intravesical instillations, and cystoscopic assessments after the survey [3]. Progression to high-grade or detrusor muscle invasive tumors is a critical issue in NMIBC management. In this study, low CRTAC1 immunoexpression correlated with high tumor grade and stage in patients with UBUC, suggesting that CRTAC1 is a potential marker of UC invasiveness. Early radical cystectomy may be advantageous for patients with NMIBC with low CRTAC1 expression. Multimodal bladder preservation treatment has been suggested for highly selected patients with MIBC [4,30]. Patients with low CRTAC1 expression in MIBC, who have a high risk of distant organ and nodal metastases, may require radical surgery. The inclusion of CRTAC1 expression in pathological parameters may help physicians select suitable candidates for bladder-preserving treatments.

UTUC is a rare genitourinary disease, accounting for 5%–10% of new UC cases. At the time of diagnosis, 60% of UTUC cases are considered invasive compared to 25%

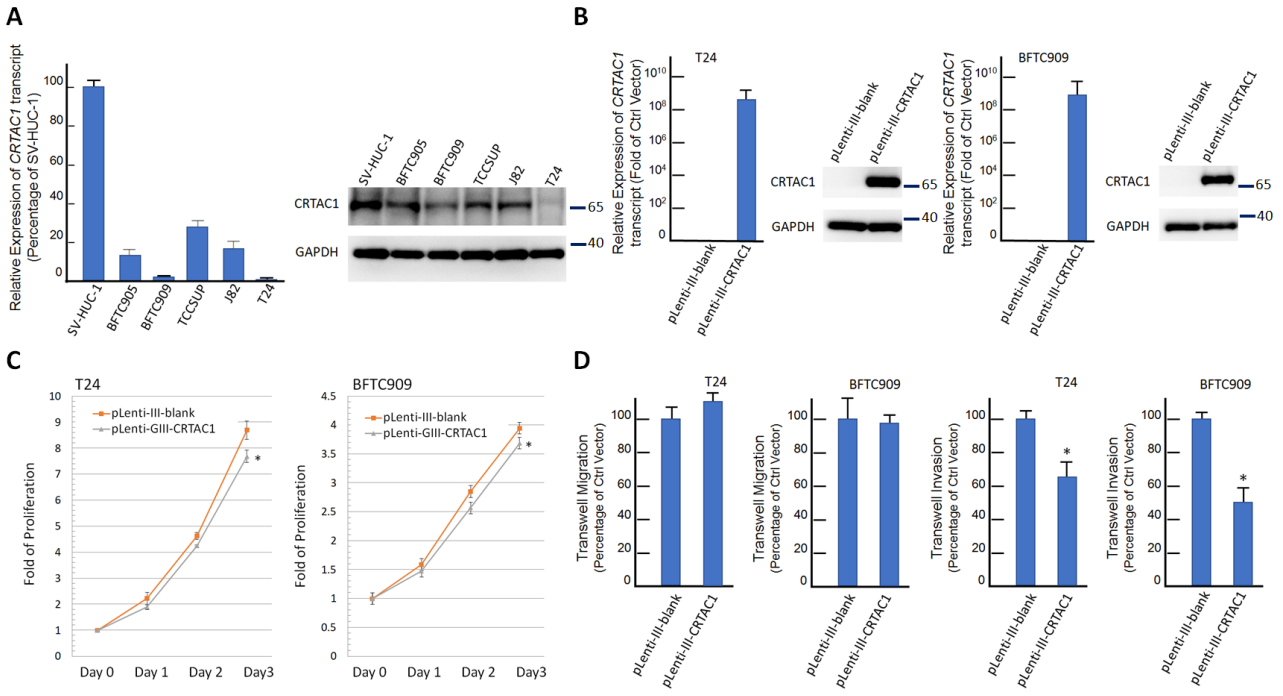

Fig. 4. CRTAC1 expression inhibits growth and invasion of UC cells *in vitro*. (A) Compared to SV-HUC-1 cells, endogenous CRTAC1 mRNA and protein expression is lower in T24 and BFTC909 cell lines. (B) CRTAC1 overexpression was induced in these two cell lines. Compared with lentiviral infection with the mock sequence, lentiviral infection with CRTAC1 significantly increased the mRNA and protein levels of CRTAC1 in BFTC909 and T24 cells. (C) The overexpression of CRTAC1 in BFTC909 and T24 cells significantly attenuates the cellular proliferation. (D) Using Transwell® migration and invasion assays, cell invasion is significantly reduced in *CRTAC1*-transfected T24 and BFTC909 cell lines, compared to that in the corresponding empty controls. (*, $p < 0.05$).

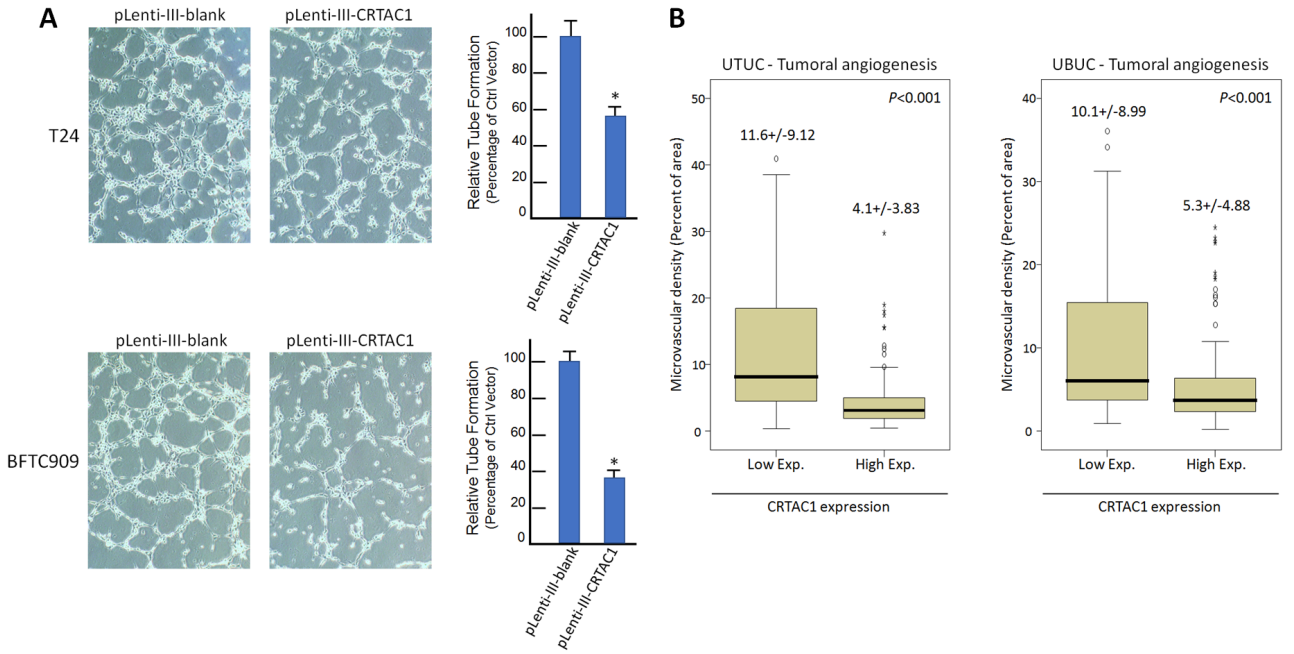

Fig. 5. CRTAC1 expression inhibits angiogenesis of UC. (A) Tube formation is markedly decreased when the HUVECs are incubated with conditioned medium from the CRTAC1-overexpressing T24 and BFTC909 cells than that from the mock groups. (B) High CRTAC1 expression is significantly correlated with less CD31-labeled microvascular density in UTUC and UBUC. (*, $p < 0.05$).

of UBUC cases [2,5]. Therefore, current guidelines recommend RNU as the standard treatment for patients with high-grade UTUC [5]. However, the benefits of lymph node dissection and its optimal extent have not yet been determined

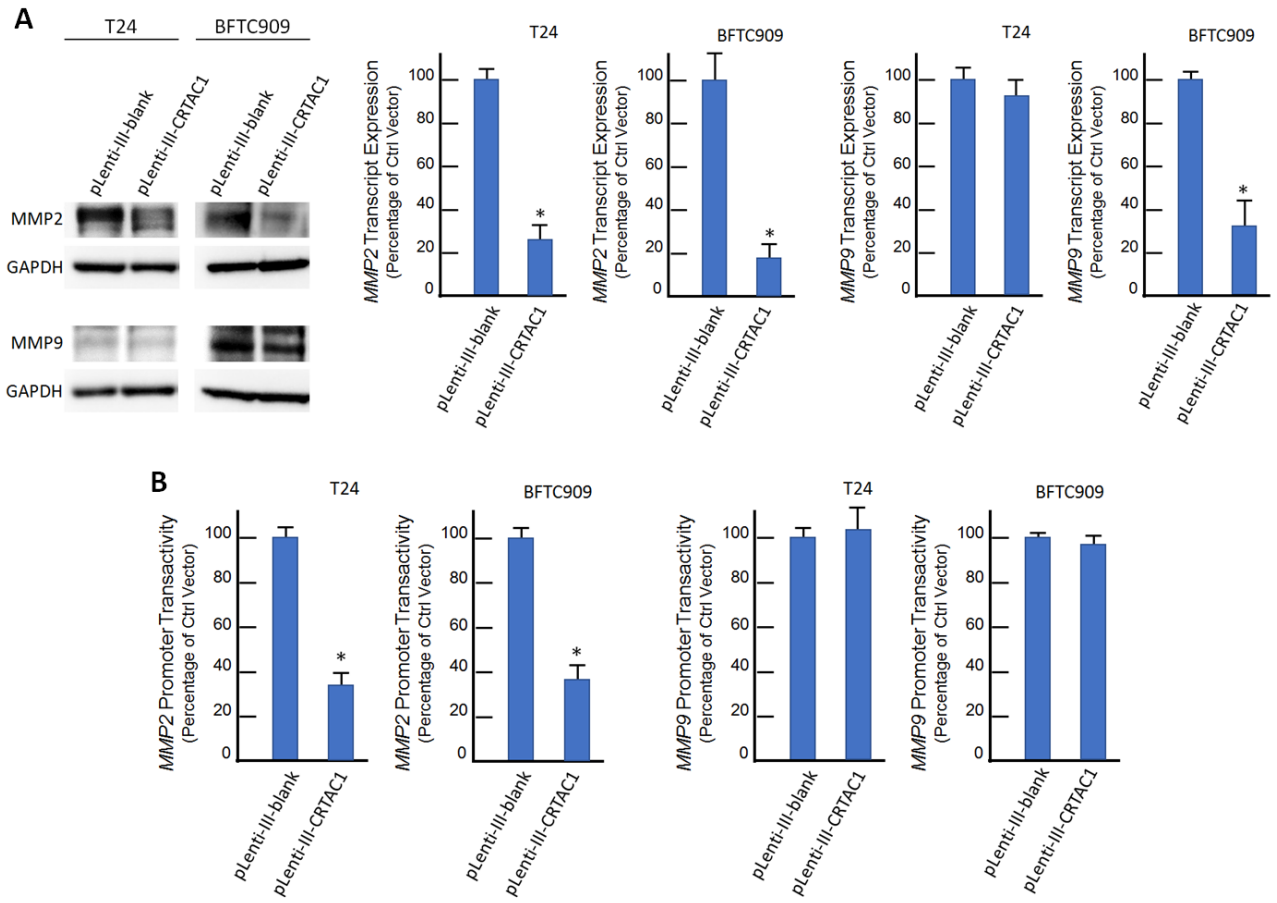

Fig. 6. CRTAC1 inhibits UC invasion by transcriptional repression of MMP2. (A) Exogenous CRTAC1 expression significantly downregulated the MMP2 mRNA and protein levels in BFTC909 and T24 cells, using qRT-PCR and western blotting. (B) The luciferase activity of *MMP2* promoter construct was significantly lower in the T24 and BFTC909 cells transfected with the *CRTAC1*-expressing vector than that in the empty controls. (*, $p < 0.05$).

in non-metastatic UTUC. In this study, low CRTAC1 expression significantly correlated with perineural invasion, vascular invasion, and nodal metastasis, resulting in poor clinical outcomes. If RNU with lymph node dissection is recommended for patients with low CRTAC1 expression, those with UTUC may be suitable candidates for this treatment. These patients are also good candidates for adjuvant chemotherapy because of the significantly high probability of subsequent metastasis. Owing to the old age, renal insufficiency, and medical comorbidities of UTUC patients, kidney-sparing management is recommended for patients with low-grade or low-stage disease [14,31]. However, accurate preoperative tumor staging is challenging. Ureteroscopic biopsy makes it difficult to obtain adequate tissue to assess invasion depth. Based on our results, aggressive features can be determined by assessing the CRTAC1 immunoexpression status in biopsy specimens. Additional information can also help achieve optimal decision making.

Letsiou *et al*. [13] elucidated the functions of *CRTAC1* in tissue biology by performing high-throughput RNA sequencing transcriptome analysis. These results demonstrated that CRATC1 regulates ECM organization in the complement cascade. The molecular mechanisms of CRTAC1 bioactivity in the wound healing process have been investigated in primary human dermal fibroblasts [14]. Gene expression analysis revealed that the CRTAC1 protein was associated with cell proliferation (downregulated CXCL12 and upregulated NOS2), cell migration (upregulated AQP3 and downregulated TNC), and extracellular matrix regeneration and remodeling (upregulated FMOD, upregulated TIMP1, downregulated FN1, and downregulated COL3A1). Similar altered genes have been found in a zebrafish skin damage repair model [32]. However, the biology of CRTAC1 in cancer remains unclear. In lung cancer, CRTAC1 expression in cancer tissues was lower than in normal tissues. Yu *et al*. [33] developed a 5-gene (*KRT6A, MELTF, IRX5, MS4A1 and CRTAC1*) signature prognostic stratification system to predict the overall survival of patients with lung cancer. In gastric cancer, low expression of CRTAC1 was strongly associated with a poor prognosis. Shen *et al*. [34] constructed a 8-gene (*KCNJ2, GATA5, CLDN1, SERPINE1, FCER2, PMEPA1, TMEM37 and CRTAC1*) survival prognosis model. They found high-risk group is more likely to escape immunity and less sensi-

tive to immunotherapy and chemotherapy [34]. In bladder cancer, Yang *et al*. [18] found that CRTAC1 overexpression inhibited cell proliferation, viability, migration, invasion and epithelial-mesenchymal transition process by downregulating Yin Yang 1 to inactivate the TGF-β pathway. In the present study, we assessed the biological functions of CRTAC1 in UC-derived cell lines. Similar to human tissues, CRTAC1 expression in UC cells was lower than that in non-tumoral urothelium. Cell proliferation, Transwell® assays, HUVEC tube formation, and immunoblotting assays showed that CRTAC1 overexpression inhibited cell proliferation, invasion, angiogenesis, and MMP2 expression. These findings are in accordance with our observation that high CRTAC1 expression was associated with low tumor stage/grade, low MVD, low incidence of UC metastasis, and better survival in our clinical cohort.

5. Conclusions

CRTAC1 expression decreases during the transition from normal urothelium to superficial and invasive UC, indicating its potential role in carcinogenesis and invasiveness. In addition, the exogenous overexpression of CRTAC1 attenuated UC-derived cell line proliferation, invasion, and angiogenesis. Therefore, CRTAC1 is a promising therapeutic target for UC. The present study also demonstrated the independent prognostic importance of CRTAC1 in survival and metastasis risk in patients with UBUC and UTUC. Therefore, close surveillance and aggressive treatments are crucial for patients with UC and low CRTAC1 levels. The addition of CRTAC1 immunostaining to routine histopathological examinations can help clinicians identify high-risk patients and facilitate individualized therapy.

Availability of Data and Materials

The datasets generated and analysed during the current study are available from the corresponding author on reasonable request.

Author Contributions

Conceptualization, WML, SCW, HLK, CCH, CFY; Data curation, TCC, WJW; Formal analysis, CFL, HLK; Investigation, WML, TCC, YCW, CFL; Methodology, WML, SCW, CFY; Supervision, CCH, SCW, CFY; Writing – original draft, WML, TCC; Writing – review & editing, YCW, CFL, HLK, WJW, CCH, SCW, CFY. All authors contributed to editorial changes in the manuscript. All authors read and approved the final manuscript.

Ethics Approval and Consent to Participate

This study was approved by the Institutional Review Board of Chi Mei Medical Center (10501005). Tissue specimens were from the BioBank of Chi-Mei Medical Center. Patient-informed consent was provided under the existing ethics approval procedures.

Acknowledgment

Not applicable.

Funding

This study was supported by Kaohsiung Medical University Hospital, Taiwan (KMUH110-0R59, KMUH111-1R56) and Ministry of Science and Technology, Taiwan (MOST109-2314-B-037-110-MY3).

Conflict of Interest

The authors declare no conflict of interest.

Supplementary Material

Supplementary material associated with this article can be found, in the online version, at https://doi.org/10.31083/j.fbl2809217.

References

[1] Siegel RL, Miller KD, Fuchs HE, Jemal A. Cancer statistics, 2022. CA: a Cancer Journal for Clinicians. 2022; 72: 7–33.

[2] Lenis AT, Lec PM, Chamie K, Mshs MD. Bladder Cancer: A Review. The Journal of the American Medical Association. 2020; 324: 1980–1991.

[3] Babjuk M, Burger M, Capoun O, Cohen D, Compérat EM, Dominguez Escrig JL, *et al*. European Association of Urology Guidelines on Non-muscle-invasive Bladder Cancer (Ta, T1, and Carcinoma in Situ). European Urology. 2022; 81: 75–94.

[4] Witjes JA, Bruins HM, Cathomas R, Compérat EM, Cowan NC, Gakis G, *et al*. European Association of Urology Guidelines on Muscle-invasive and Metastatic Bladder Cancer: Summary of the 2020 Guidelines. European Urology. 2021; 79: 82–104.

[5] Rouprêt M, Babjuk M, Burger M, Capoun O, Cohen D, Compérat EM, *et al*. European Association of Urology Guidelines on Upper Urinary Tract Urothelial Carcinoma: 2020 Update. European Urology. 2021; 79: 62–79.

[6] Cancer Genome Atlas Research Network. Comprehensive molecular characterization of urothelial bladder carcinoma. Nature. 2014; 507: 315–322.

[7] Necchi A, Madison R, Pal SK, Ross JS, Agarwal N, Sonpavde G, *et al*. Comprehensive Genomic Profiling of Upper-tract and Bladder Urothelial Carcinoma. European Urology Focus. 2021; 7: 1339–1346.

[8] Clapham DE. Calcium signaling. Cell. 2007; 131: 1047–1058.

[9] Wu L, Lian W, Zhao L. Calcium signaling in cancer progression and therapy. The FEBS Journal. 2021; 288: 6187–6205.

[10] Elíes J, Yáñez M, Pereira TMC, Gil-Longo J, MacDougall DA, Campos-Toimil M. An Update to Calcium Binding Proteins. Advances in Experimental Medicine and Biology. 2020; 1131: 183–213.

[11] Worcester EM. Urinary calcium oxalate crystal growth inhibitors. Journal of the American Society of Nephrology. 1994; 5: 46–53.

[12] Steck E, Bräun J, Pelttari K, Kadel S, Kalbacher H, Richter W. Chondrocyte secreted CRTAC1: a glycosylated extracellular matrix molecule of human articular cartilage. Matrix Biology. 2007; 26: 30–41.

[13] Letsiou S, Manchado M, Zografaki M, Marka S, Anjos L, Skliros D, *et al*. Deciphering the role of cartilage protein 1 in human dermal fibroblasts: a transcriptomic approach. Functional & Integrative Genomics. 2021; 21: 503–511.

[14] Letsiou S, Félix RC, Cardoso JCR, Anjos L, Mestre AL, Gomes HL, *et al*. Cartilage acidic protein 1 promotes increased cell vi-

ability, cell proliferation and energy metabolism in primary human dermal fibroblasts. Biochimie. 2020; 171–172: 72–78.
[15] Sun Y, Rong X, Li D, Jiang Y, Lu Y, Ji Y. Down-regulation of CRTAC1 attenuates UVB-induced pyroptosis in HLECs through inhibiting ROS production. Biochemical and Biophysical Research Communications. 2020; 532: 159–165.
[16] Sun Y, Rong X, Li D, Lu Y, Ji Y. NF-κB/Cartilage Acidic Protein 1 Promotes Ultraviolet B Irradiation-Induced Apoptosis of Human Lens Epithelial Cells. DNA and Cell Biology. 2020; 39: 513–521.
[17] Ge X, Ritter SY, Tsang K, Shi R, Takei K, Aliprantis AO. Sex-Specific Protection of Osteoarthritis by Deleting Cartilage Acid Protein 1. PLoS ONE. 2016; 11: e0159157.
[18] Yang J, Fan L, Liao X, Cui G, Hu H. CRTAC1 (Cartilage acidic protein 1) inhibits cell proliferation, migration, invasion and epithelial-mesenchymal transition (EMT) process in bladder cancer by downregulating Yin Yang 1 (YY1) to inactivate the TGF-β pathway. Bioengineered. 2021; 12: 9377–9389.
[19] He J, Dong C, Zhang H, Jiang Y, Liu T, Man X. The oncogenic role of TFAP2A in bladder urothelial carcinoma via a novel long noncoding RNA TPRG1-AS1/DNMT3A/CRTAC1 axis. Cellular Signalling. 2023; 102: 110527.
[20] Wang H, Li J, Zi X, Yuan X. Comprehensive analysis of cuproptosis-related genes on bladder cancer prognosis, tumor microenvironment invasion, and drug sensitivity. Frontiers in Oncology. 2023; 13: 1116305.
[21] Sjödahl G, Lauss M, Lövgren K, Chebil G, Gudjonsson S, Veerla S, *et al*. A molecular taxonomy for urothelial carcinoma. Clinical Cancer Research. 2012; 18: 3377–3386.
[22] Chan TC, Li CF, Ke HL, Wei YC, Shiue YL, Li CC, *et al*. High TNFAIP6 level is associated with poor prognosis of urothelial carcinomas. Urologic Oncology. 2019; 37: 293.e11–293.e24.
[23] Li CF, Chan TC, Wang CI, Fang FM, Lin PC, Yu SC, *et al*. RSF1 requires CEBP/β and hSNF2H to promote IL-1β-mediated angiogenesis: the clinical and therapeutic relevance of RSF1 overexpression and amplification in myxofibrosarcomas. Angiogenesis. 2021; 24: 533–548.
[24] Chan TC, Chen YT, Tan KT, Wu CL, Wu WJ, Li WM, *et al*. Biological significance of MYC and CEBPD coamplification in urothelial carcinoma: Multilayered genomic, transcriptional and posttranscriptional positive feedback loops enhance oncogenic glycolysis. Clinical and Translational Medicine. 2021; 11: e674.
[25] Liang PI, Yeh BW, Li WM, Chan TC, Chang IW, Huang CN, *et al*. DPP4/CD26 overexpression in urothelial carcinoma confers an independent prognostic impact and correlates with intrinsic biological aggressiveness. Oncotarget. 2017; 8: 2995–3008.
[26] Wang YH, Wu WJ, Wang WJ, Huang HY, Li WM, Yeh BW, *et al*. CEBPD amplification and overexpression in urothelial carcinoma: a driver of tumor metastasis indicating adverse prognosis. Oncotarget. 2015; 6: 31069–31084.
[27] Anjos L, Morgado I, Guerreiro M, Cardoso JCR, Melo EP, Power DM. Cartilage acidic protein 1, a new member of the beta-propeller protein family with amyloid propensity. Proteins. 2017; 85: 242–255.
[28] Anjos L, Gomes AS, Melo EP, Canário AV, Power DM. Cartilage Acidic Protein 2 a hyperthermostable, high affinity calcium-binding protein. Biochimica et Biophysica Acta. 2013; 1834: 642–650.
[29] Ji Y, Rong X, Li D, Cai L, Rao J, Lu Y. Inhibition of Cartilage Acidic Protein 1 Reduces Ultraviolet B Irradiation Induced-Apoptosis through P38 Mitogen-Activated Protein Kinase and Jun Amino-Terminal Kinase Pathways. Cellular Physiology and Biochemistry. 2016; 39: 2275–2286.
[30] Ghandour R, Singla N, Lotan Y. Treatment Options and Outcomes in Nonmetastatic Muscle Invasive Bladder Cancer. Trends in Cancer. 2019; 5: 426–439.
[31] Marcq G, Foerster B, Abufaraj M, Matin SF, Azizi M, Gupta M, *et al*. Novel Classification for Upper Tract Urothelial Carcinoma to Better Risk-stratify Patients Eligible for Kidney-sparing Strategies: An International Collaborative Study. European Urology Focus. 2022; 8: 491–497.
[32] Félix RC, Anjos L, Costa RA, Letsiou S, Power DM. Cartilage Acidic Protein a Novel Therapeutic Factor to Improve Skin Damage Repair? Marine Drugs. 2021; 19: 541.
[33] Yu P, Tong L, Song Y, Qu H, Chen Y. Systematic profiling of invasion-related gene signature predicts prognostic features of lung adenocarcinoma. Journal of Cellular and Molecular Medicine. 2021; 25: 6388–6402.
[34] Shen Y, Chen K, Gu C. Identification of a chemotherapy-associated gene signature for a risk model of prognosis in gastric adenocarcinoma through bioinformatics analysis. Journal of Gastrointestinal Oncology. 2022; 13: 2219–2233.